Nigerian Journal of Physics (NJP)
ISSN online: 3027-0936
ISSN print: 1595-0611
DOI: https://doi.org/10.62292/njp.v35i4.2026.591
Volume 35(4), December 2026

Performance Evaluation of Satellite Gravity on Variable Test Points and Geophysical Models in Gongola Basin, Nigeria

***Adamu Aliyu Bagare**

Department of Physics, Yobe State University, Nigeria.

*Corresponding Author's Email: dr.addamu@gmail.com

Keywords:
Aeromagnetic,
Gongola,
Forward Modelling,
Gravity,
Satellite.

Submitted: 25 May 2026

Accepted: 15 June 2026

Published: 22 July 2026

ABSTRACT

The recent advent of new satellite missions provides models of gravity data with high quality and global coverage that is on par with conventional gravity measurements. A drawback is the myriad of models to choose from and the number of test points to use for validation. As a result, an accuracy assessment needs to be performed to isolate the best model. Therefore, this paper compared 21 satellite models at varying testing points. Furthermore, the best gravity model was assessed based on 2-D (Two-Dimensional) geophysical modeling constrained by the aeromagnetic survey. XGM2019e_2159 gravity model attained the highest performance indicator value from the quantitative analysis of the Gongola Basin. It has an RMSE (0.847861), MAE (4.102917), RMSPE (14.24%), MAPE (12.24%) and highest correlation (0.847861) with the terrestrial Bouguer anomalies, for this reason, it is deemed most suitable for the application of this research. Overall, based on the mean accuracy of the whole set of points, the best six (6) satellite models in decreasing accuracy are XGM2019e-2159, XGM2016, GECO, EGM-2008, EIGEN-6C4 and GGM05C. Generally, a set of data points might perform better than another set, one should use as much available data set for selecting the best model ensuring the data sets are well distributed across the research area. The satellite data performed slightly better than the terrestrial data based on the geophysical modeling by a discrepancy of ±2 mGal. Generally, a set of data points might perform better than another set, therefore one should use as much available data set for selecting the best model ensuring the data sets are well distributed across the research area.

INTRODUCTION

Gravity investigation is one of the prominent geophysical procedures employed in delineating the earth's interior (Despotovic et al., 2016). Gravity potential can be measured via Satellite, airborne, Shipborne, or ground also known as terrestrial method. Terrestrial gravity is the traditional method of data acquisition that usually produces a scanty network of points during gravity surveys (Šprlák et al., 2011). This is due to the tediousness of the methods used and in some hard-to-reach areas such as mountainous regions, it is next to impossible to collect such data (Eyike et al., 2010). As a result, airborne surveys were used to collect the potential of such provinces. Although Data captured on the ground (terrestrial), sea (shipborne) and airplane (airborne) are highly accurate making them crucial for constructing a global gravity field, the data observed via these procedures typically have scarce coverage, prolonged periods, and absence of recurrent observations, deeming it impossible for global coverage at appropriate cost (Pouliquen et al., 2017). Therefore, Satellite provided an alternative for capturing gravity data. Satellite gravity models find application in various domains, including fault and discontinuity identification and crustal modelling. In addition, oceanic geological structure, mineral resource accumulation, oil and gas presence can be inferred from satellite gravity measurements (Abdallah et al., 2022; Apeh et al., 2018; Balmino et al., 2012; DOĞRU, 2021; Eyike et al., 2010; Hirt et al., 2013; Maghfira & Windhi Niasari, 2019; Pouliquen et al., 2017; Putri et al., 2019; Vu et al., 2019).

The accomplishment of the Radar Altimeter measurements in 1978, initiated the concept for satellite gravity measurements (Yılmaz et al., 2010). This fundamentally altered the geophysicists' and geodesists' understanding of tectonic processes, which in turn allowed for the computation of several global gravity fields utilizing new satellite missions. As a result, new satellite missions were used to calculate different global gravity fields, drastically altering the knowledge of tectonic processes held by geophysicists and geodesists (Odera, 2016). Recently due to its high resolution and data accessibility, satellite altimetric missions have emerged as a crucial instrument for establishing regional and global gravity data as technological advancements have continued to progress (Huang & Véronneau, 2009). The gravity field models are calculated at different precisions from numerous Satellites leading to several models of varying accuracies suitable for different applications. As such the accuracies of these satellite gravity models needed to be verified with terrestrial data (Barthelmes, 2013; Despotovic et al., 2016; Karunasingha, 2022; Wang & Lu, 2018). Several studies have been carried out across the globe to determine the accuracy of satellite gravity models using terrestrial data (Balmino et al., 2012; Huang & Véronneau, 2009; Odera, 2016; Saari & Biljer-Koivula, 2017; Šprlák et al., 2011; Yılmaz et al., 2010). All the cited research used a fixed number of terrestrial observations to measure the precision of the gravity models in which they reported different accuracies. The variation in the accuracy of the gravity models may be due to the difference in regions or the number of observation points used. Therefore, this research varies the number of observation points to assess its effect on the performance of some selected gravity models. Moreover, the use of RMSE (Root Mean Square Error) by previous research in the assessment of model accuracy has a deficiency of penalizing outliers, since geophysical surveys are not free from outliers, few outliers might render a good model poor, therefore we suggest RMSE to be complimented by MAE (Mean Absolute Error) as MAE gives the absolute error without penalizing outliers. Furthermore, (Pouliquen et al., 2017) model gravity satellite without constraining it to any complementing geophysical method which usually produces a non-unique solution. To minimize the non-uniqueness, this research employs high resolution aeromagnetic data to constrain the model.

The research therefore used both qualitative and quantitative approaches to compare the terrestrial gravity data collected from BGI (Gravimetrique International Bureau) (http://bgi.omp.obsmip.fr) for Gongola Basin in Nigeria, with the global gravity anomalies acquired from the ICGEM (International Centre for Global Earth Models) (http://icgem.gfz-potsdam.de/ICGEM). To identify the best gravity model, the gravity model exhibiting the least MAE and RMSE that coincide with the Highest correlation coefficient was chosen as the best model. In addition, a subsurface performance evaluation was also carried out between the terrestrial gravity and the best satellite gravity model with aeromagnetic data.

Geology and Location of the Study Area

In northeastern Nigeria, Gongola branch of the Upper Benue Trough is situated between longitude 10.00° E to 12.50° E and latitude 9.50° N to 11.50° N. Gongola basin encompasses Basement rocks of Precambrian era, sedimentary sequences of Cretaceous to Recent era and volcanics of Tertiary era (Olakunle & Abdulmumin, 2019). The basement rocks encompassing the study area, particularly those that are exposed, belong to the Older Granite group, which also includes mylonites, granodiorites, and granites. Starting from the youngest the sedimentary sequences have Kerri-Kerri as the topmost underlined by Gombe, Pindiga, Yolde and Bima Formations (Figure. 1). The Gongola basin's stratigraphy, geology, and tectonic development have all been thoroughly recorded by (Abubakar et al., 2010; Salako & Udensi, 2015; Shemang et al., 2005) among other authors.

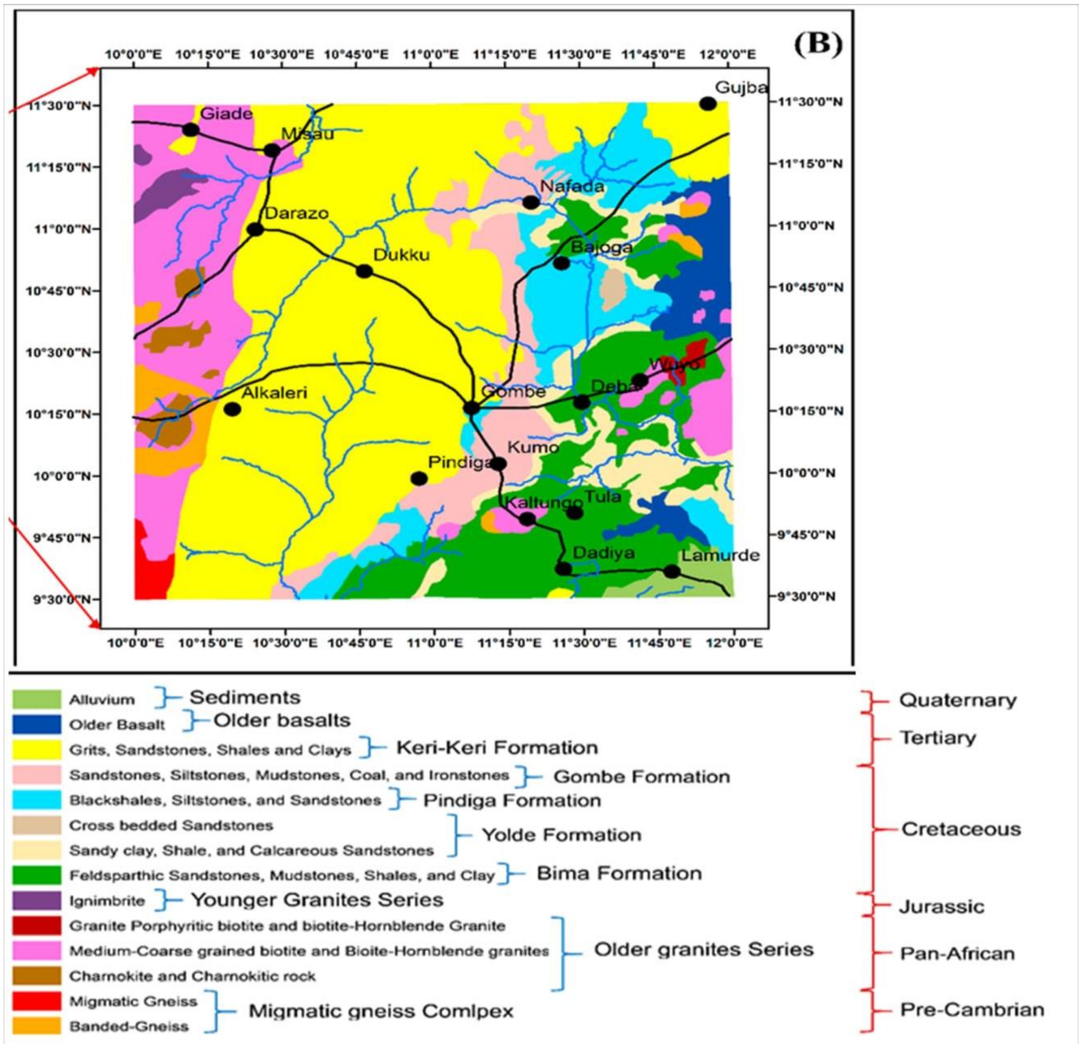

Figure 1: Geology of the Study Area Modified from Yusuf et al., (2021)

Correlation

Correlation is a method of quantifying the relationship between two variables. The relationship is in a form of either positively correlated (same variation) or negatively correlated (opposite variation). The phrase "correlation" is frequently referred to a linear relationship Pearson product moment correlation between continuous variables (Schober & Schwarte, 2018).

$$r = \frac{n\sum jk - \sum j \sum k}{\sqrt{[n\sum j^2 - (\sum j)^2][n\sum k^2 - (\sum k)^2]}} \quad (1)$$

Where r is the Perasons correlation coeffieient, j and k are the values of variables which in our case are the terrestrial ang satellite gravity values.

RMSE and RMSPE

The RMSE measures the degree to which these residuals are scattered, providing insight into how well the observed data adheres to the expected values. When the RMSE values is low, it signifies that the model has more precise estimates and matches the observation well. While larger RMSE values, signifies superior error and poor estimates. In every case, RSME exceeds or equals MAE (RSME >= MAE). The larger disparity between them suggests a higher variation in the sample's individual mistakes (Kambezidis, 2012).

$$RMSE = \sqrt{\left[\frac{1}{N}\sum_{i=1}^{N}(H_{mi} - H_{ei})^2\right]} \quad (2)$$

Where H_e and H_m are the terrestrial bouguer anomaly and the satellite bouguer anomaly respectively. i represents measured pair of individual values and N represents the total no of measurements.

Sometimes RMSE is expressed in percentage referred to as RMSPE (Root Mean Square Percentage Error) (Kambezidis, 2012).

$$RMSE = \frac{\sqrt{\left[\frac{1}{N}\sum_{i=1}^{N}(H_{mi} - H_{ei})^2\right]}}{\frac{1}{N}\sum_{i=1}^{N}H_{mi}} \quad (3)$$

MAE and MAPE

MAE stands for mean absolute error between observed and anticipated values. The row-level error computation known as MAE, or L1 loss, computes the non-negative difference between the actual and the prediction. The formula for calculating MAE is (Despotovic et al., 2016).

$$MAE = \frac{1}{N}\sum_{i=1}^{N}|(H_{mi} - H_{ei})| \quad (4)$$

When stated as a percentage, the MAE is sometimes referred to as mean absolute percentage error (MAPE) (Despotovic et al., 2016).

$$MAPE = \frac{1}{N}\sum_{i=1}^{N}\left|\frac{(H_{mi}-H_{ei})}{H_{mi}}\right| \quad (5)$$

2D Forward Modelling

A forward model calculates an anomaly from a hypothetical geologic model, compares it to the anomaly observed, and makes manual tunings to the model to enhance the comparison. Until the modeller is pleased with the outcome, the procedure is repeated. In a 2-D (Two-Dimensional) model the earth is considered to vary in x and z directions while in a 2.75-D has a limited range of distance in the Y direction. Oasis Montaj's GM-SYS profile is algorithm used in the determination of the magnetic and gravity feedback from a geologic model. The techniques employed to determine the response of the magnetic and gravity models are based on the techniques of (Talwani et al., 1959). The foundation for computations in two-and-a-half dimensions was based on (Rasmussen & Pedersen, 1979). The 2D equation for gravity is given by (Blakely, 1996).

$$g(p) = 2G\rho \iint \frac{zdxdz}{x^2+z^2} \quad (6)$$

MATERIALS AND METHODS

Various software ware used in the processing of the terrestrial gravity, satellite gravity model and aeromagnetic data. These includes Oasis Montaj for the correction, processing and forward of the gravity data. Surfer 17 and Microsoft excel were also utilized in this research for plotting of graphs and images superimposition respectively. In addition, Surfer 17 they were also used to exchange data in different formats. Q GIS was used in the digitization of the geologic and location map.

Terrestrial Gravity

The Terrestrial Gravity gravity observation points was sourced from BGI (Gravimetrique International Bureau) (http://bgi.omp.obsmip.fr). It consists of 236 data points which were dispersed within the entire research area. courtesy of the data goes to British Antarctic Survey, Geological Survey of Nigeria, University of Ibadan Nigeria (Depart. of Geology) and Geophysical Survey of The Southwestern Part of The Chad Basin.

Satellite Gravity Models

The satellite gravity data test points were sourced from International Centre for Global Earth Models (ICGEM) (Sinem Ince et al., 2019). The preferred gravity data obtained from ICGEM were EGM 2008, EIGEN-6C4, GECO, XGM2019e-2159, EIGEN-CG03c, XGM2016, GIF48, GGM05S, GGM05G, GGM05C, GFZ97, GEMT3s, GEM10a, GAO2012, EIGEN- GRGS.RL04, EIGEN-GRACE02S, EIGEN, GL04S1, EIGEN-CHAMP05S, AIUB-GRACE03S, DEOS_CHAMP-01C and DGM-1S.

Aeromagnetic

The aeromagnetic data of Gongola Basin comprising of Sixteen (16) high resolution aeromagnetic maps was sourced from the NGSA (Nigeria Geological Survey Agency). The maps encompass of sheet numbers 107, 108, 109, 110, 129, 130,131,132, 150,151,152,153, 171,172, 173 and 174 which covers longitudes 10.00^0 E to 12.00^0 E and latitudes 9.50^0 N to 11.50^0 N.

Procedure

The initial stage involves importing the satellite gravity models into excel followed by comparison of each satellite model with terrestrial gravity based on the RMSE, RMSPE, MAE, MAPE and Pearsons correlation coefficient. Six of the best Performing models were then selected and their accuracies based on varying number of observation points was evaluated. The best performing model was the model with least RMSE and MAE over the entire five varying observation points. The final chosen satellite model was imported to Oasis Montag for modelling. The procedure started by invoking the GMSYS from the (GX's) Geosoft Executables menu followed by the creation of database for the profiles. The profiles were selected approximately orthogonal to the strike of the major anomalies and geological units of the Gongola basin. further procedures for joint forward modelling of gravity and magnetics include the incorporation of the magnetic and sedimentary contact across the profile. This was modelled to minimize error.

RESULTS AND DISCUSSION

Residual Bouguer Anomaly

For the terrestrial data, the residual Bouguer anomaly ranges from -13.2 mGal to 12.1 mGal (Figure 2a). The colour bar shows where there is a strong density contrast below the surface, represented by regions of red and pink; intermediate values, represented by green and yellow; and low-density contrast, represented by blue. Comparably, (Figure 2b) of the satellite gravity model displays a range of 11.0465 mGal to -16.1077 mGal for the residual bouguer anomaly. Furthermore, its colour bar indicates low gravity (blue colour) and intermediate values (green and yellow) that correlate to low density contrast areas; and regions with high gravity (red and pinks) that correspond to regions with high density contrast below the surface.

Residual Magnetic Anomaly Reduced to the Equator (RTE) Map

The RTE map represents a transformation of the anomaly over the source. It shows a varying intensity of 110.2 nT to −141.5 nT. The colour bar was used to split the research area into three magnetic zones, each of which has a distinct magnetic anomaly pattern (Figure 2c). The magnetic characteristics of the underlying rock types are primarily responsible for this magnetic zoning. The first zone encompasses the centre, northeastern, and southwest regions of the study area. It is underlain by crystalline foundation rocks from the Precambrian period with high susceptibility based on the geology of the area. With amplitudes of magnetic intensity classified as moderate on the colour legend bar, the second zone is deemed intermediate (positive) anomalies. The characteristic that stands.ut the most on the map is the third zone. It has magnetic abnormalities that are primarily negative to barely positive, this constitutes the sedimentary zones.

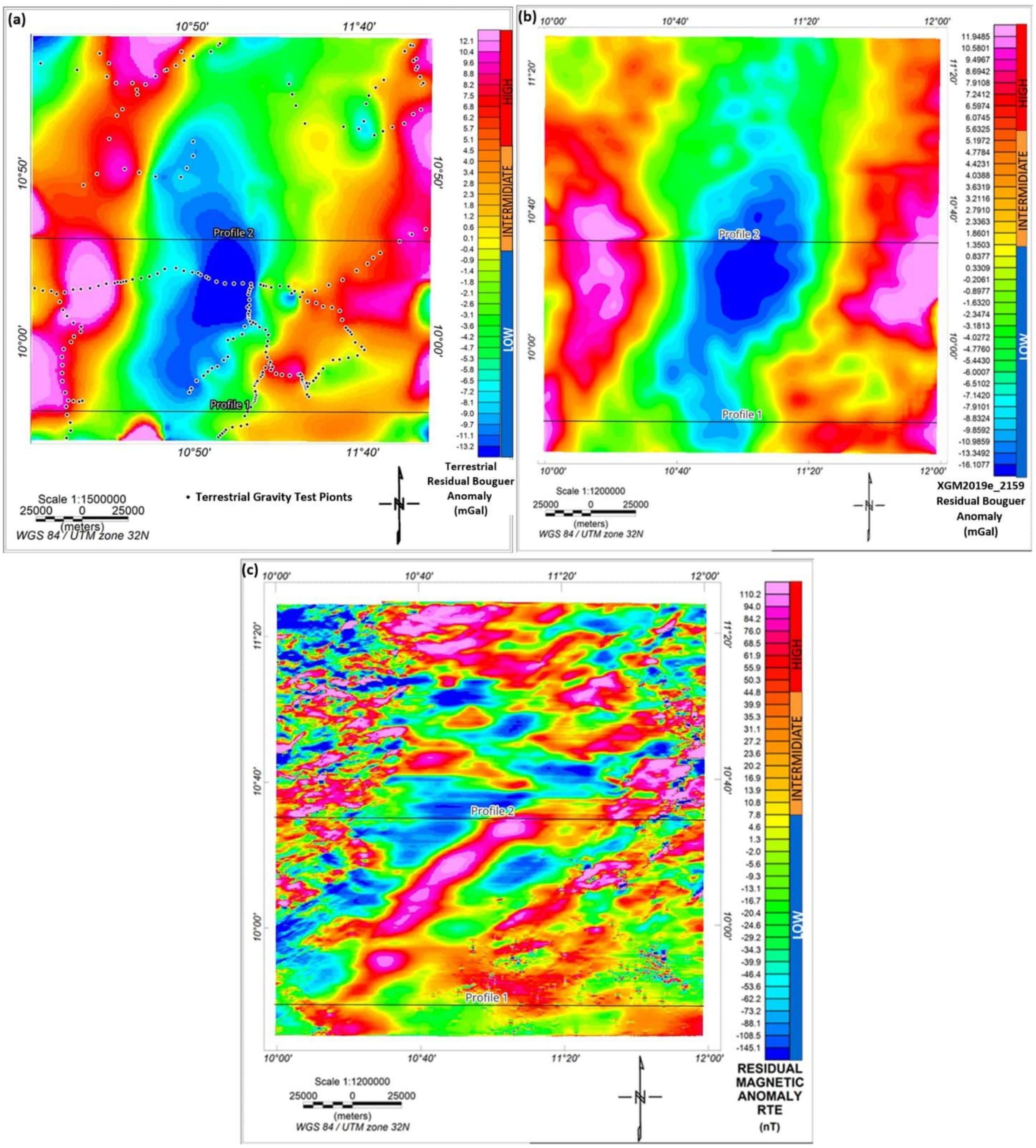

Figure 2: Potential Field Maps (a) Terrestrial Gravity (b) Satellite Gravity XGM 2019e_2159 (c) Aeromagnetic

Qualitative Analysis

Figure 3 a to g shows the bouguer anomaly maps of the terrestrial and satellite gravity models. The figure qualitatively assesses the relationship between the terrestrial bouguer and satellite gravity models. The terrestrial gravity (Figure 3a) shows a huge depression in colour (weak anomaly) at the centre which was the signature anomaly compared with the satellite gravity models. EGM 2008 (Figure 3b) matches the signature anomaly of Figure 3a at the bottom half but suffers from strong positive anomaly intrusion towards the upper half of the map, which makes a moderate fit in comparison to Figure 3a. Eigen 6C4 and GECO also exhibit a very good fit with the signature anomaly of Figure 3a but surfers from a moderate intrusion of a strong anomaly, these two Satellite bouguer gravity models were classified as good. XGM 2019e_2159 shows a superb fit with the signature anomaly of Figure 3a, only a mild trace of strong anomaly could be seen making it the excellent model in the configuration. XGM 2016 has a good fit with the signature anomaly, but the orientation was off, which also makes it a good fit. GGM50C has the weakest fit with the signature anomaly in the configuration, even though it fit at the bottom half of the map like Figure 3b, it connects two strong anomalies at the top making it stand out.

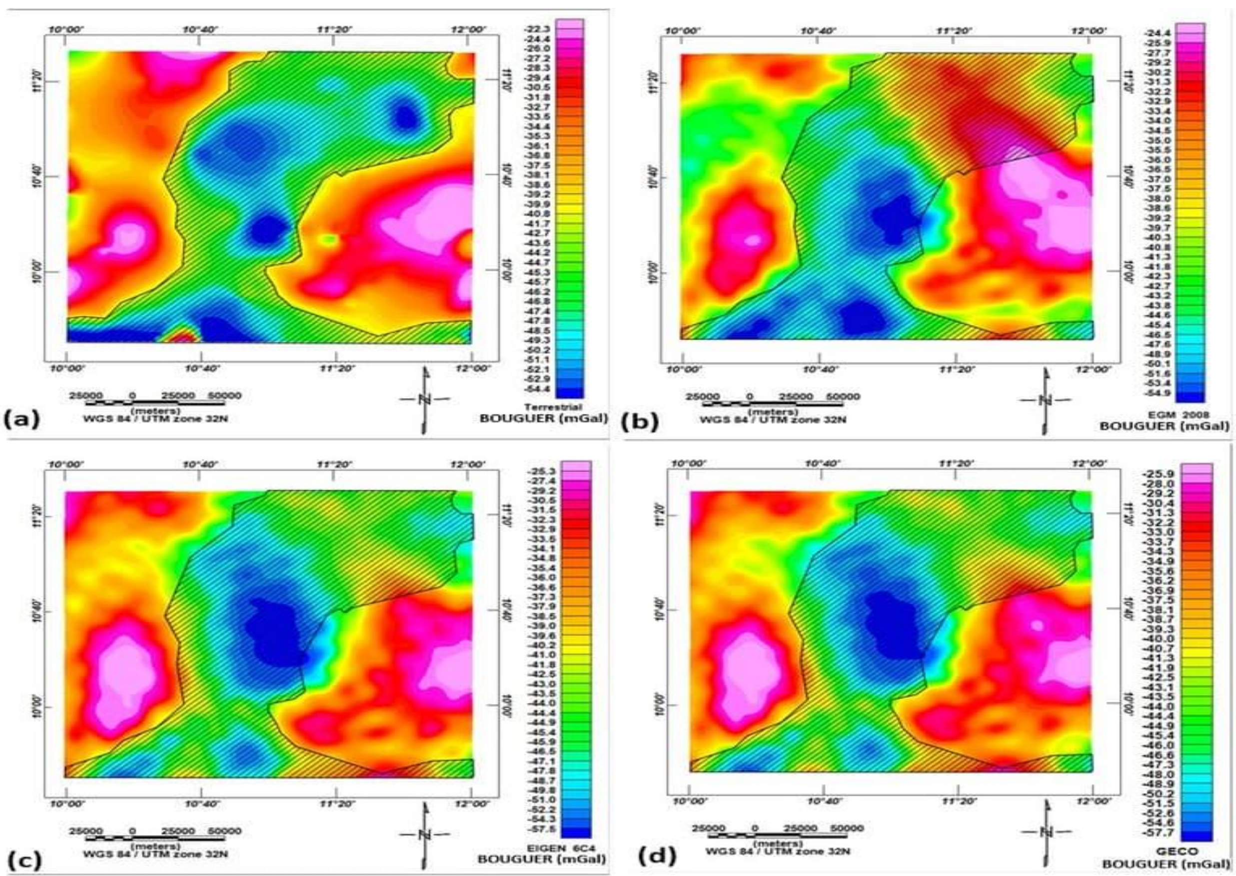

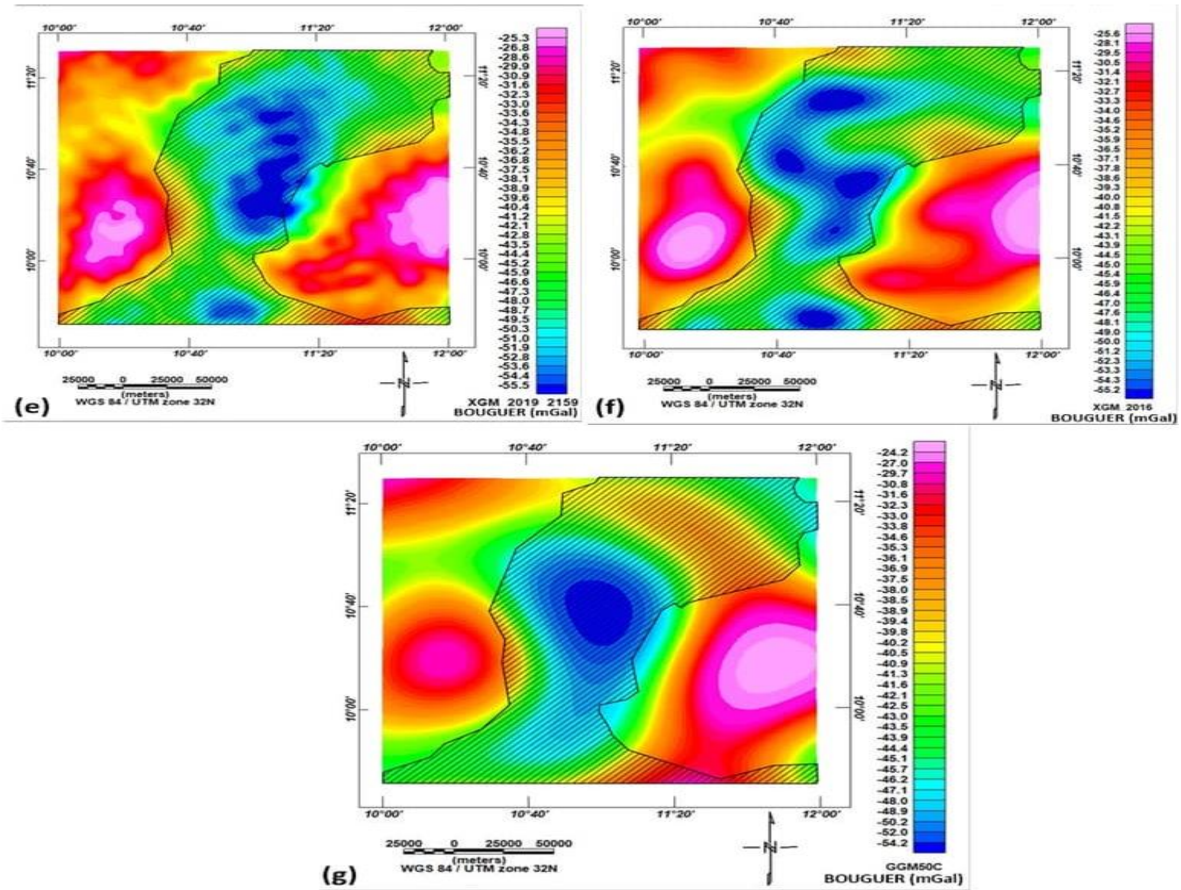

Figure 3: Terrestrial Bouguer Anomalies Against Satellite Derived Bouguer Anomalies

Quantitative Analysis Based on Variable Test Points

It is evident from Table (2) and Figure (4) that the performance of the satellite gravity models is better at some regions of points than others. As such the performance of each of the best six models selected from Table (1) were analysed statistically with varying the number of points as indicated in Figure 4a through 4e. Starting with only 30 test points, XGM2019e_2159 was the best model. It has a corresponding value of RMSE, MAE, MAPE, RMSPE and R-value of 2.590206, 2.118982, 6.70%, 7.11% and 0.966614. Consequently, GGM05C was the least Model. Adjusting to 60 test points, EGM 2008 was the best model with values of RMSE, MAE, MAPE, RMSPE and R-value associated with 5.731533, 3.972022, 12.07%, 15.75% and 0.852908, whereas EIGEN-6C4 was the least model. At 120 test points, XGM 2016 has RMSE, MAE, MAPE, RMSPE and R-value of 5.329694, 4.321852, 12.63%, 13.64% and 0.872792 respectively. EGM 2008 which was the best model at 60 points is now the least model, this shows that the number of points can profoundly alter the accuracy of a model thereby misleading a researcher into choosing a less overall model. The best model at 180 point and 235 point is XGM2019e_2159 while the least performing model is EIGEN-6C4.

Table 1: Cumulative Statistical Result of the Varying Test Points for Satellite Derived Bouguer Anomalies

SN	Satellite Gravity Model	RMSE (mGal)	MAE (mGal)	MAPE	RMSPE	R-Value
1	EGM 2008	6.425333	4.539769	13.30%	17.01%	0.773494
2	EIGEN-6C4	6.506012	4.995249	14.87%	17.25%	0.809028
3	GECO	6.179399	4.610792	13.84%	16.38%	0.817067
4	XGM2019e-2159	5.377842	4.102917	12.24%	14.24%	0.847861
5	EIGEN-CG03c	11.31965	9.266458	25.59%	30.20%	0.665152
6	XGM2016	5.848519	4.624064	14.05%	15.53%	0.832336
7	GIF48	7.626849	5.77634	17.08%	20.27%	0.719285
8	GGM05S	12.98975	9.926768	30.95%	34.54%	-0.12509

SN	Satellite Gravity Model	RMSE (mGal)	MAE (mGal)	MAPE	RMSPE	R-Value
9	GGM05G	7.868947	6.27552	20.15%	20.92%	0.731914
10	GGM05C	6.532483	4.993825	14.92%	17.34%	0.771651
11	GFZ97	9.286085	7.724299	21.57%	24.72%	0.690662
12	GEMT3s	23.96156	21.59639	54.18%	63.64%	-0.12801
13	GEM10a	11.5543	9.680994	30.01%	30.73%	0.011169
14	GAO2012	8.580376	6.708466	20.12%	22.86%	0.668949
15	EIGEN- GRGS.RL04	6.754827	5.178158	15.39%	17.92%	0.740834
16	EIGEN-GRACE02S	17.15393	14.22359	41.42%	45.67%	-0.32895
17	EIGEN-GL04S1	11.43851	9.213099	29.85%	30.45%	-0.24793
18	EIGEN-CHAMP05S	14.94525	11.55082	38.39%	39.84%	-0.33148
19	AIUB-GRACE03S	9.888335	8.079765	26.61%	28.41%	0.621435
20	DEOS_CHAMP-01C	11.48438	9.557137	30.08%	30.54%	-0.10255
21	DGM-1S	9.034792	6.973519	22.44%	24.00%	0.52076

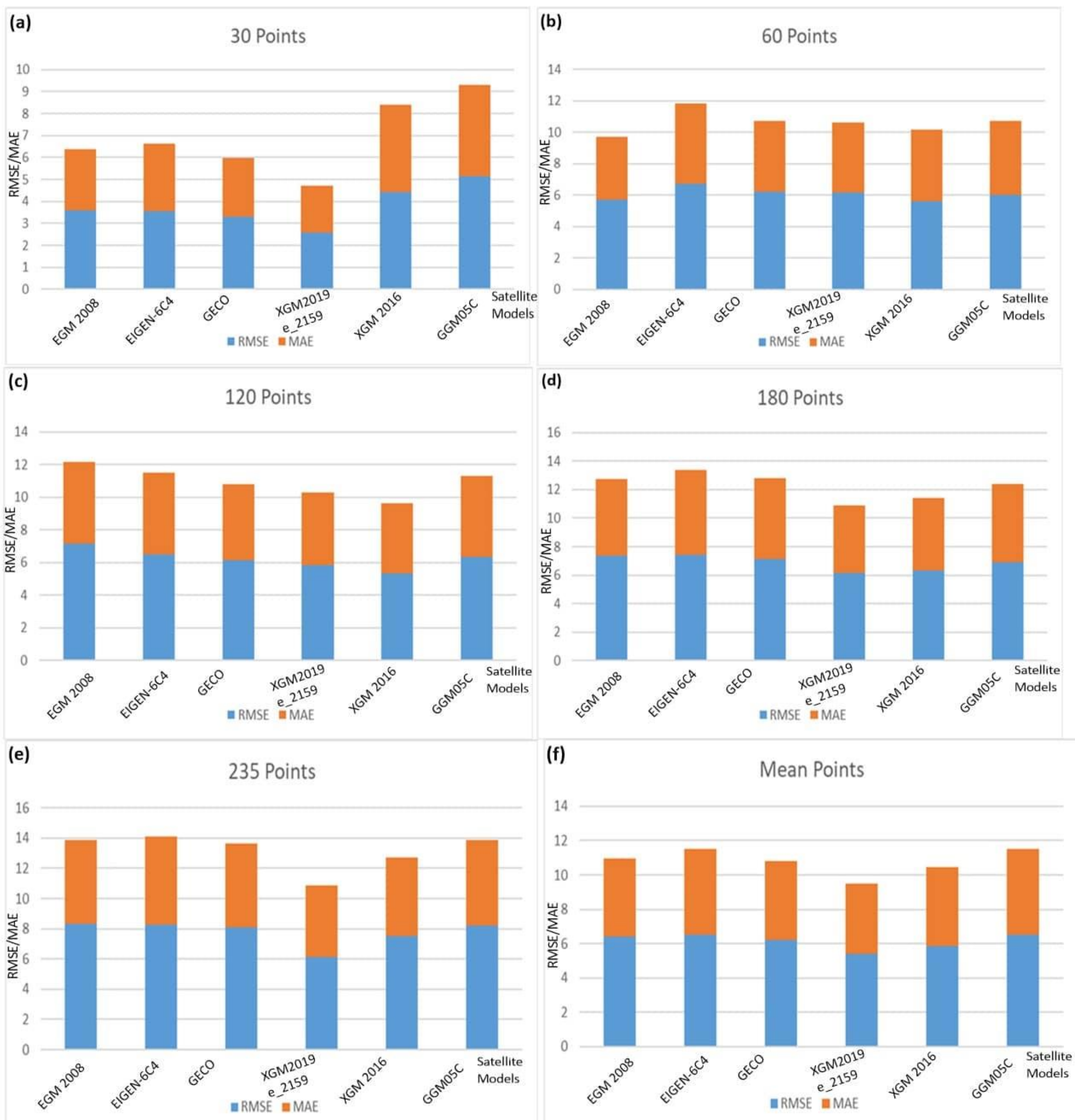

Figure 4: Stacked Column Chart of RMSE and MAE

Overall, based on the mean accuracy of the whole set of points, the six (6) satellite models in decreasing accuracy are XGM2019e-2159, XGM2016, GECO, EGM-2008, EIGEN-6C4 and GGM05C. It can be noticed that the error increases with increasing number of points, this is due to higher variations towards the end of our data points, as such taking the average provide the overall best model.

Table 2: Terrestriel Bouguer Anomalies vs Satellite Bouguer Models

Satellite Gravity Model	Parameters	235 Points	180 Points	120 Points	60 Pionts	30 Pionts	Mean
EGM 2008	RMSE	8.31775	7.33765	7.133049	5.731533	3.606685	6.425333
	MAE	5.537216	5.382871	5.023707	3.972022	2.783025	4.539769
	MAPE	16.67%	15.35%	13.35%	12.07%	9.05%	13.30%
	RMSPE	21.91%	19.23%	18.26%	15.75%	9.90%	17.01%
	R-Value	0.6289	0.684543	0.743355	0.852908	0.957766	0.773494
EIGEN-6C4	RMSE	8.282837	7.434853	6.495701	6.747095	3.569574	6.506012
	MAE	5.847185	5.956048	5.008307	5.098062	3.066643	4.995249
	MAPE	17.82%	17.62%	14.35%	14.85%	9.69%	14.87%
	RMSPE	21.82%	19.49%	16.63%	18.54%	9.79%	17.25%
	R-Value	0.696431	0.761803	0.822267	0.81583	0.948812	0.809028
GECO	RMSE	8.083516	7.152641	6.16084	6.204208	3.295788	6.179399
	MAE	5.579596	5.645086	4.626047	4.526128	2.677103	4.610792
	MAPE	17.08%	16.78%	13.32%	13.31%	8.73%	13.84%
	RMSPE	21.29%	18.75%	15.77%	17.05%	9.04%	16.38%
	R-Value	0.704141	0.774322	0.836911	0.82198	0.947982	0.817067
XGM2019e-2159	RMSE	6.13515	6.150338	5.834977	6.178541	2.590206	5.377842
	MAE	4.709583	4.759078	4.462864	4.464076	2.118982	4.102917
	MAPE	14.26%	14.21%	12.75%	13.26%	6.70%	12.24%
	RMSPE	16.05%	16.12%	14.94%	16.98%	7.11%	14.24%
	R-Value	0.787025	0.816508	0.850612	0.818546	0.966614	0.847861
XGM2016	RMSE	7.528324	6.336909	5.329694	5.615786	4.431884	5.848519
	MAE	5.196357	5.068686	4.321852	4.556176	3.977248	4.624064
	MAPE	16.15%	15.31%	12.63%	13.71%	12.45%	14.05%
	RMSPE	19.83%	16.61%	13.64%	15.43%	12.16%	15.53%
	R-Value	0.718829	0.806962	0.872792	0.837061	0.926036	0.832336
GGM05C	RMSE	8.201025	6.926084	6.360443	6.026833	5.14803	6.532483
	MAE	5.687896	5.490894	4.964287	4.677973	4.148077	4.993825
	MAPE	17.32%	16.06%	13.79%	14.44%	13.00%	14.92%
	RMSPE	21.60%	18.16%	16.28%	16.56%	14.12%	17.34%
	R-Value	0.632503	0.730672	0.798645	0.804607	0.891827	0.771651

Modelling

The parameters obtained from profile 1 includes a susceptibility contrast of 0.3 SI unit for the upper basement and 0.0123 SI unit for the lower basement corresponding to a density of 2.65 and 2.67 respectively. A depth of 4778.68 m and 13693.95 m was observed corresponding to bottom and Conrad depth for the respective upper and lower basement. The crystalline basement surfaced at the extreme West and Eastern part where the basement depth is shallowest. The analysis of joint forward modelling also reveals five sedimentary horizons with an approximate thickness 4778.68 m maximum. The first strata (Kerri-Kerri) have a mean depth of 372.9083 m and a density of 2.4 gcc. Beneath Kerri-Kerri is Gombe strata with a slightly higher density of 2.45 gcc and a mean depth of 589.1915 m. Pindiga formation succeeds Gombe with a relatively higher density of 2.57 gcc and average depth of 831.87 m. Yolde and Bima both have a density of 2.47 gcc with Yolde having a mean depth of 952.7705 m and Bima 1537.578 m. The best fit acceptable model of the satellite data has a susceptibility root mean square error of 8.985 for the Magnetic signal and 1.515 for the Gravity survey (Figure 5a). This is a consequent of the heterogeneity involved with magnetic surveys. The best fit acceptable model of the terrestrial data has a susceptibility root mean square error of 8.985 for the Magnetic signal and 3.161 for the Gravity survey (Figure 5b). This is due to interpolation of large gaps in sparse data points.

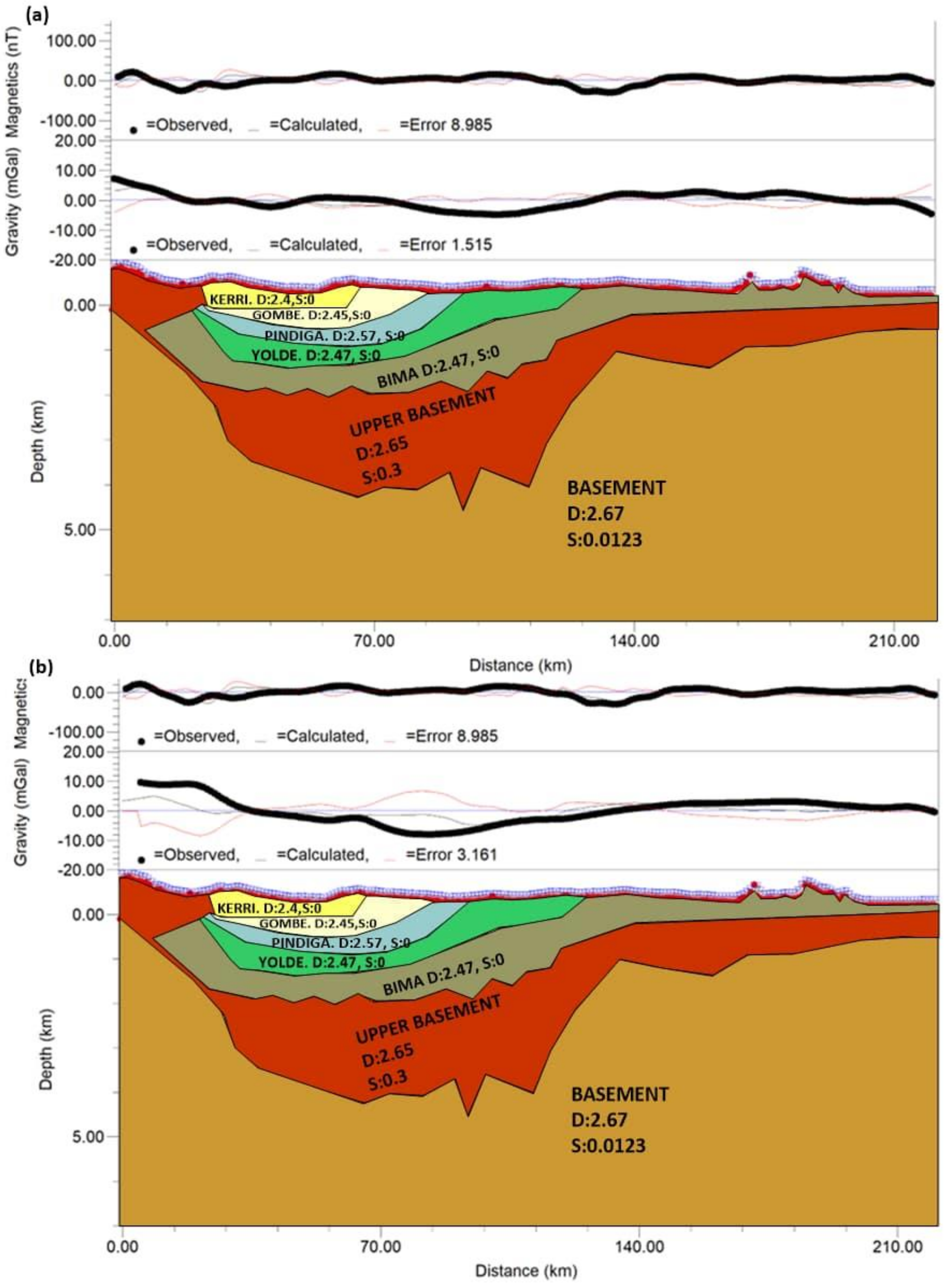

Figure 5: Profile 1 Model

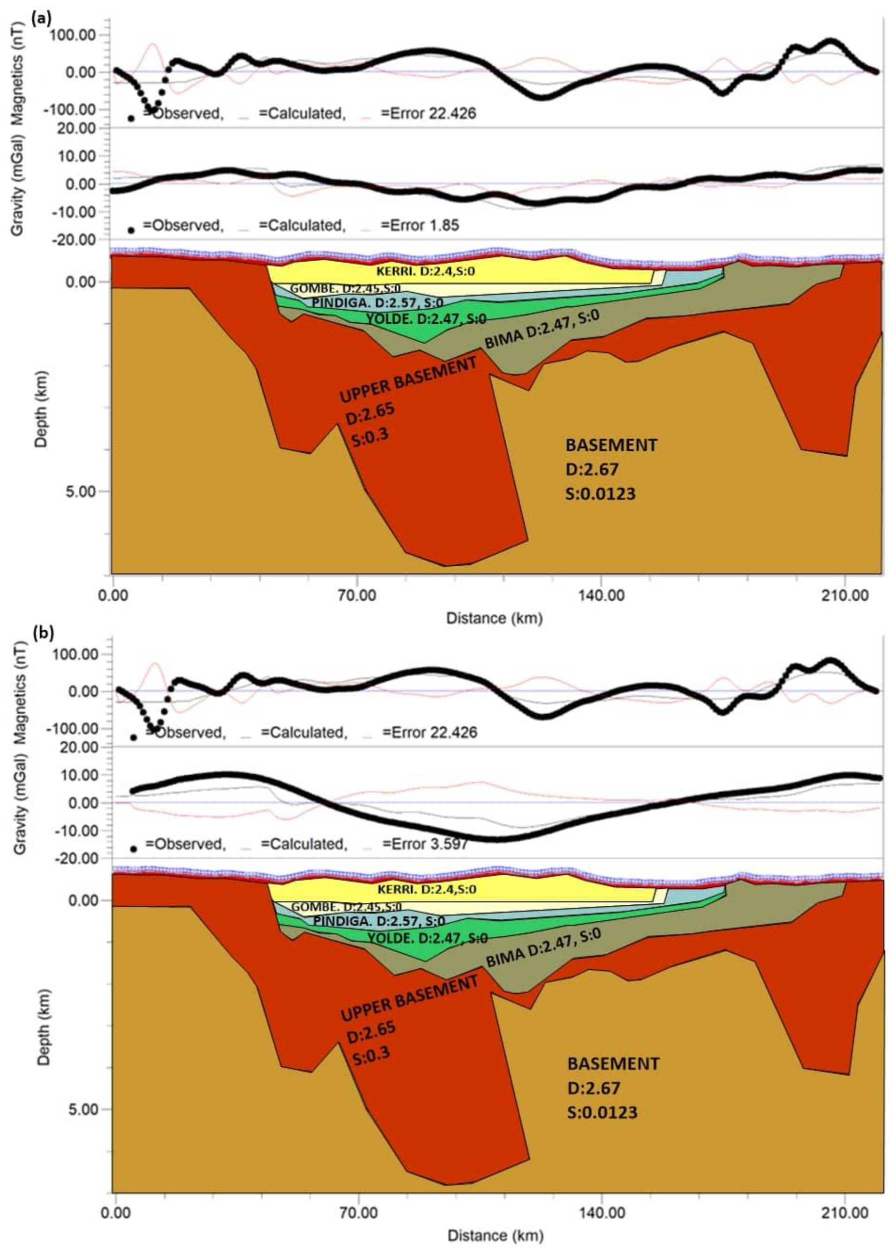

Figure 6: Profile 2 Model

Profile 2 illustrates the model top of Precambrian bedrock and sedimentary thickness obtained from 2.75-dimensional coupled gravity and aeromagnetic survey. A good root mean square fit of 1.85 for gravity survey and a moderate fit of 22.426 for the aeromagnetic survey was obtained which correspond to the satellite data (Figure 6a). Whereas a 3.597 value was obtained for the terrestrial data (Figure 6b). The depth to bottom of the upper bedrock elevations range from less than 650.38 m above the topography in the extreme ends of the profile to 7248.15m in the central region of the profile. This suggests a huge depression at the centre and uplift at the west and eastern ends associated with a density of 2.65 gcc and a magnetic susceptibility of 0.31 SI. The lower bedrock shows some moderate undulations and has a depth to bottom of 13583.32 m with a susceptibility value of 0.0123 and density value of 2.67 gcc. The sedimentary cover was modelled on top of the bedrock with a thickness of 2336.4 m. This is a relatively shallow in comparison with the previous profiles. Kerri-Kerri layer yields a minimum density of 2.4 gcc and an average depth of 375.6564 m, while at a mean distance of 528.8992 m and a density of 2.45 gcc lay Gombe formation. Pindiga formation has a mean depth of 738.1333 and moderate density of 2.57 gcc. Yolde and Bima formations are the last layers in the succession with a density of 2.47 gcc.

They have a corresponding mean depth of 1057.904 m and 1330.492 m which is also relatively low compared to the profiles that preceded it.

CONCLUSION

The research evaluates and validate the accuracy of satellite gravity models using terrestrially observed Bouguer anomalies at two hundred and thirty five (235) test points in Gongola Basin, Nigeria. The lowest performance indicators value was obtained from the XGM2019e_2159 model as a result of the quantitative study for the Gongola Basin. It has an RMSE (0.847861), MAE (4.102917), RMSPE (14.24%), MAPE (12.24%) and highest correlation (0.847861) with the terrestrial bouguer anomalies, for this reason, it is deemed most suitable for the application of this research. Overall, based on the mean accuracy of the whole set of points, the six (6) satellite models in decreasing accuracy are XGM2019e-2159, XGM2016, GECO, EGM-2008, EIGEN-6C4 and GGM05C. It can be noticed that the error increases with an increasing number of points, this is due to higher variations towards the end of our data, as such taking the average provides the overall best model. Generally, a set of data points might perform better than others set, therefor one should use as much available data set for selecting the best model ensuring the data sets are well distributed across the research area.

REFERENCES

Abdallah, M., Abd El Ghany, R., Rabah, M., & Zaki, A. (2022). Comparison of recently released satellite altimetric gravity models with shipborne gravity over the Red Sea. *Egyptian Journal of Remote Sensing and Space Science*, *25*(2), 579–592. https://doi.org/10.1016/j.ejrs.2022.03.016

Abubakar, Y., Umegu, M., & Ojo, S. (2010). Evolution of Gongola Basin Upper Benue Trough Northeastern Nigeria. . . *Asian J. Earth Sci.*, *3*(2), 62–67. www.academicjournals.com

Apeh, O. I., Moka, E. C., & Uzodinma, V. N. (2018). Evaluation of gravity data derived from global gravity field models using terrestrial gravity data in Enugu State, Nigeria. *Journal of Geodetic Science*, *8*(1), 145–153. https://doi.org/10.1515/jogs-2018-0015

Balmino, G., Vales, N., Bonvalot, S., & Briais, A. (2012). Spherical harmonic modelling to ultra-high degree of Bouguer and isostatic anomalies. *Journal of Geodesy*, *86*(7), 499–520. https://doi.org/10.1007/s00190-011-0533-4

Blakely, R. J. (1996). *POTENTIAL THEORY IN GRAVITY AND MAGNETIC APPLICATIONS*. Cambridge University Press.

Despotovic, M., Nedic, V., Despotovic, D., & Cvetanovic, S. (2016). Evaluation of empirical models for predicting monthly mean horizontal diffuse solar radiation. In *Renewable and Sustainable Energy Reviews* (Vol. 56, pp. 246–260). Elsevier Ltd. https://doi.org/10.1016/j.rser.2015.11.058

DOĞRU, F. (2021). Comparison of Recent and Former Satellite-Based Gravity Models: A Case Study of Kansas, USA. *Deu Muhendislik Fakultesi Fen ve Muhendislik*, *23*(69), 835–844. https://doi.org/10.21205/deufmd.2021236911

Eyike, A., Werner, S. C., Ebbing, J., & Dicoum, E. M. (2010). On the use of global potential field models for regional interpretation of the West and Central African Rift System. *Tectonophysics*, *492*(1–4), 25–39. https://doi.org/10.1016/j.tecto.2010.04.026

Hirt, C., Claessens, S., Fecher, T., Kuhn, M., Pail, R., & Rexer, M. (2013). New ultrahigh-resolution picture of Earth's gravity field. *Geophysical Research Letters*, *40*(16), 4279–4283. https://doi.org/10.1002/grl.50838

Huang, J., & Véronneau, M. (2009). Evaluation of the Grace-based Global Gravity Models in Canada. *N Bull*, *4*, 3–17.

Kambezidis, H. D. (2012). 3.02 - The Solar Resource. In *Comprehensive Renewable Energy* (pp. 27–84). Elsevier. https://doi.org/10.1016/B978-0-08-087872-0.00302-4

Karunasingha, D. S. K. (2022). Root mean square error or mean absolute error? Use their ratio as well. *Information Sciences*, *585*, 609–629. https://doi.org/10.1016/j.ins.2021.11.036

Maghfira, P. D., & Windhi Niasari, S. (2019). Gravity satellite data analysis for subsurface modelling in Mount Merapi-Merbabu, Java, Indonesia. *E3S Web of Conferences*, *76*. https://doi.org/10.1051/e3sconf/20197603003

Odera, P. A. (2016). Assessment of EGM2008 using GPS/leveling and free-air gravity anomalies over Nairobi County and its environs. *South African J Geo.*, *51*, 17–30. https://doi.org/http://dx.doi.org/10.4314/sajg.v5i1.2.

Olakunle, O., & Abdulmumin, Y. (2019). Journal of African Earth Sciences Basement configuration and lineaments mapping from aeromagnetic data of Gongola arm of Upper Benue Trough , northeastern Nigeria. *Journal of African Earth Sciences*, *160*, 1–13. https://doi.org/10.1016/j.jafrearsci.2019.103597

Pouliquen, G., Connard, G., Kearns, H., Gouiza, M., & Paton, D. (2017). Public domain satellite gravity inversion offshore Somalia combining layered-Earth and 3 voxel based modelling. *FIRST BREAK* , *3*(5). http://eprints.whiterose.ac.uk/121050/

Putri, D. R., Nanda, M., Rizal, S., Idroes, R., & Ismail, N. (2019). Interpretation of gravity satellite data to delineate structural features connected to geothermal resources at Bur Ni Geureudong geothermal field. *IOP Conference Series: Earth and Environmental Science*, *364*(1). https://doi.org/10.1088/1755-1315/364/1/012003

Rasmussen, R., & Pedersen, L. B. (1979). End Corrections in Potential Field Modeling. *Geophysical Prospecting*, *27*, 740–760.

Saari, T., & Biljer-Koivula, M. (2017). Evaluation of GOCE-based Global Geoid Models in Finnish Territory. *EGU General Assembly Conference Abstracts*.

Salako, K., & Udensi, E. (2015). Two dimentional modeling of subsurface structure over upper Benue trough and Bornu basin in North eastern Nigeria. *Nigerian Journal of Technological Research*, *10*(1), 94. https://doi.org/10.4314/njtr.v10i1.s11

Schober, P., & Schwarte, L. A. (2018). Correlation coefficients: Appropriate use and interpretation. *Anesthesia and Analgesia*, *126*(5), 1763–1768. https://doi.org/10.1213/ANE.0000000000002864

Shemang, E. M., Jacoby, W. R., & Ajayi, C. O. (2005). Gravity Anomalies Over the Gongola Arm, Upper Benue Trough, Nigeria. *Global Journal of Geological Sciences*, *3*(1), 61–69.

Sinem Ince, E., Barthelmes, F., Reißland, S., Elger, K., Förste, C., Flechtner, F., & Schuh, H. (2019). ICGEM – 15 years of successful collection and distribution of global gravitational models, associated services, and future plans. *Earth System Science Data*, *11*(2), 647–674. https://doi.org/10.5194/essd-11-647-2019

Šprlák, M., Pettersen, B. R., Šprlák, M., Gerlach, C., & Omang, O. C. D. (2011). *Comparison of GOCE Derived Satellite Global Gravity Models with EGM2008, the OCTAS Geoid and Terrestrial Gravity Data: Case Study for Norway*. https://www.researchgate.net/publication/258490479

Talwani, M., Worzel, J. L., & Landisman, M. (1959). Rapid Gravity Computations for Two-Dimensional Bodies with Applications to the Mendocino Submarine Fracture Zones. *Journal of Geophysical Research*, *64*, 49–59.

Vu, D. T., Bruinsma, S., & Bonvalot, S. (2019). A high-resolution gravimetric quasigeoid model for Vietnam. *Earth, Planets and Space*, *71*(1). https://doi.org/10.1186/s40623-019-1045-3

Wang, W., & Lu, Y. (2018). Analysis of the Mean Absolute Error (MAE) and the Root Mean Square Error (RMSE) in Assessing Rounding Model. *IOP Conference Series: Materials Science and Engineering*, *324*(1), 1–10. https://doi.org/10.1088/1757-899X/324/1/012049

Yılmaz, I., Yılmaz, M., & Turgut, B. (2010). Evaluation of recent global geopotential models based on GPS/levelling data over Afyonkarahisar (Turkey). *Sci. Res. and Essays*, *5*(5), 484–493.

Yusuf, A., San, L. H., & Abir, I. A. (2021). A preliminary geothermal prospectivity mapping based on integrated GIS, remote-sensing, and geophysical techniques around northeastern Nigeria. *Sustainability (Switzerland)*, *13*(15). https://doi.org/10.3390/su13158525